Behaviour of Laterally Loaded Pile

S. Ahayan
ArGEnCo Departement
University of Liège, Belgium
Institut de Recherche en Génie Civil et Mécanique (GeM)
École Centrale Nantes, France

B. Cerfontaine, F. Collin
ArGEnCo Departement
University of Liège, Belgium

P. Kotronis
Institut de Recherche en Génie Civil et Mécanique (GeM)
École Centrale Nantes, France

ABSTRACT: Monopiles have been by far the most common support structure for offshore turbines. They have always been an appropriate solution for complex site conditions.
Design of monopiles is usually based on the use of nonlinear p-y curve. These curves are primordially based on the use of simple constitutive models for soil, such as Tresca criterion. Since soil behavior is highly non-linear and very complex, fundamental features of soil such as anisotropy, creep, or destructuration have to be taken into consideration. Accordingly, it is necessary to consider more complex soil behavior constitutive models. This work aims to explain, via FEM simulations, the influence of different constitutive laws for soil, on the laterally loaded pile responses. Tresca, Mohr-Coulomb criteria and Modified Cam-Clay model have been compared and their effect on p-y curve is analyzed.

1 INTRODUCTION

Offshore wind energy applications have great potential towards achieving European Unions energy target for 2020. Accordingly, in the last decade, there is an exponential increase in the offshore wind energy industry. Offshore Wind Turbines (OWT) substructure is an important concern. This is due to the huge construction cost of the foundations and substructures, which counts for 25 to 30% of the total construction cost (EWEA 2015). Larger wind parks are increasingly developed away from the coastline, at increasing water depths. Current projects reach a distance of $150Km$ offshore and at a water depth up to $45m$. The scale of online wind farms follows an upward trend since the early 2000s, and is correlated to the rising size and production capacity of individual windmills. In the last 25 years, the energy production of one single OWT has been increased twentyfold, while rotor diameter has been grown from $35m$ up to more than $150m$ (Schaumann, Lochte-Holtgreven, & Steppeler 2011). The continuous increase of OWT dimensions attests the rapid growth of the offshore wind market.

The type and design of the foundation solutions for OWT projects depend on the size of the turbine, water depth, and local seabed conditions. According to those constraints, the challenge is to develop the most cost-effective solution for the support structure and onsite installation process (Arshad & OKelly 2013). The support structure of OWT comprises the substructure on the top of the foundation system. On one hand, the substructure is chosen based on the mean sea level. On the other hand, the foundation type is bonded to the OWT dimensions, transfer of applied loads to the soil, and ground geotechnical properties.

In a shallow and moderate water depth, between $10m$ and $70m$, the use is made of bottom-mounted substructures that are firmly fixed to the seabed by underwater foundations. Three main layouts are commonly used for shallow OWT applications: monopod, multipod, and jacket structure. Additionally, there are three practical options for the foundation system, comprising the gravity base foundations (GBF), piled foundations, and the skirt or bucket foundations, also

known as suction caissons foundations.

Based on the database of The European Wind Energy Association (EWEA) for the year 2016, it shows that 88% of the installed substructure foundation systems in Europe used monopiles, whereas the remaining 12% corresponded to jacket structures. In this research, the focus is made on offshore wind turbine based on single piles, which are designed to resist lateral loading, such as wind, wave and rotor reactions.

P-y curve is one of the most common methods that has been widely used (API (RP2A-WSD 2000), DNV (Veritas 2004),ect). P-y curves represent the relationship between the lateral load (p) and lateral displacement (y) at a certain point of a pile. Several numerical techniques, such as finite element and finite difference methods, are employed to predict the p-y curve for laterally loaded pile design (Byrne, McAdam, Burd, Houlsby, Martin, Zdravkovi, Taborda, Potts, Jardine, & Sideri 2015), (Zdravković, Taborda, Potts, Jardine, Sideri, Schroeder, Byrne, McAdam, Burd, Houlsby, et al. 2015)).

The work of Matlock (Matlock 1970) is widely used by the offshore pile industry. Matlocks recommendations are primordially based on the use of simple constitutive models for soil, meaning elastic perfectly plastic model such as Tresca or Mohr- Coulomb criteria. Since the behaviour of the clay soil is highly nonlinear and very complex, it is necessary to consider advanced constitutive models (Ahayan, Yin, Kotronis, & Collin 2016). This research aims to explain, via FEM simulations, the influence of using different constitutive laws of the soil on the responses of laterally loaded piles. Those laws vary from the simplest model, such as Tresca, to the critical state law of Cam-Clay model (Roscoe & Burland 1968). The effect of each model on the prediction of p-y curve is presented in the following sections.

2 FINITE ELEMENT MODEL

The finite element model presented in this section allows analysing pile behaviour under lateral monotonic loading. The main objective is to assess the influence of soil behaviour on the p-y curve.

The p-y curve method considers the pile as a beam, while the soil is considered as a series of uncoupled non-linear springs (Reese, Cox, & Koop 1974). Each of those springs are defined by a p-y curve, as shown in Figure 1.

The non-linear finite element code LAGAMINE, developed at the University of Liege (Collin 2003), is selected as the main numerical platform for this study.

2D simulation of laterally loaded pile

In the present work, the 3D problem of laterally loaded pile is simplified to a 2D problem to determine the characteristic p-y curve by numerical modeling. This simplification takes place by considering a slice

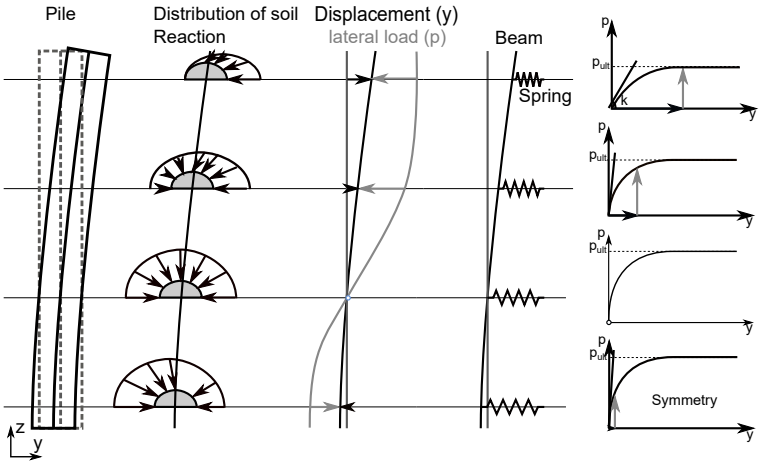

Figure 1: The p-y curve method

of one meter-wide soil at a given depth and by assuming plane strain conditions, as illustrated in Figure 2. Similar assumption can be found in (Zhang, Ye, Noda, Nakano, & Nakai 2007).

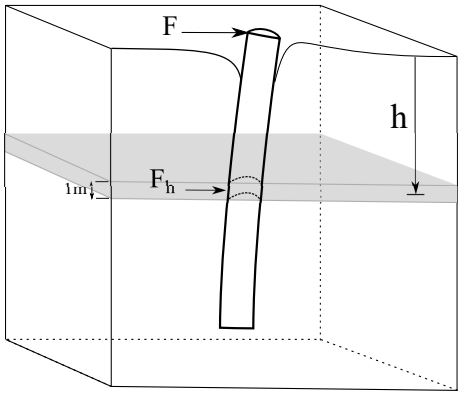

Figure 2: From 3D to 2D representation of laterally loaded pile problem

Geometry and boundary conditions

Representative dimensions are set for an offshore monopile of $2m$ diameter. Figure 4 shows the model dimensions and the considered mesh. Since the pile is assumed to be submitted to a symmetrical lateral loads, only half of the pile is simulated.

Pile loading

Monopile, as an offshore substructure, is designed to resist mainly to cyclic lateral loads, coming from wind, wave and rotor solicitations. However, the most critical influence of the cyclic loads occurs during the first cycles. Therefore, the investigation has been conducted for the first cyclic loads on the offshore monopile.

In the following, the analysis is carried out by applying a lateral displacement equivalent to 10% of the pile diameter to ensure that the lateral bearing capacity of the soil is reached. Lateral displacement is unloaded afterwards to reach its initial position, and applied again on the negative direction with the same

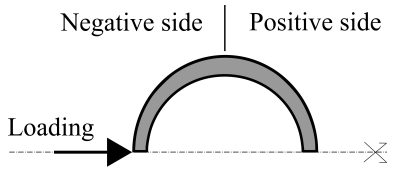

Figure 3: Loading pile configuration

value (see Figure 3). Based on this displacement, a large deformation has to be considered, in addition to gapping between the the pile and the soil.

FE Mesh

The pile section is considered as a rigid body, and the soil matrix is discretized using 3040 quadrangular (8 nodes) elements.

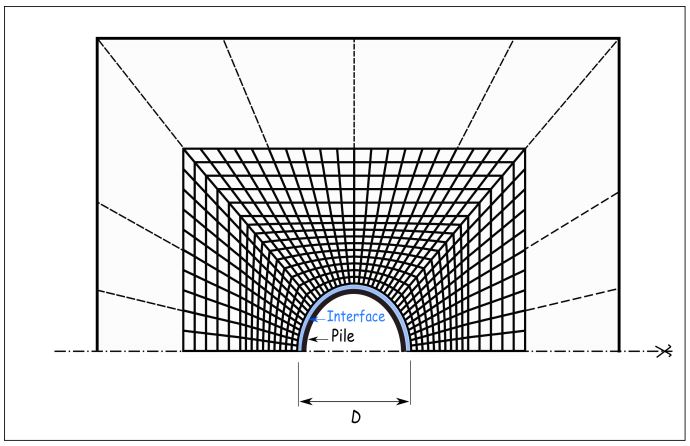

Figure 4: 2D finite element model

As a consequent of lateral displacement forces, a gap is created between the soil and the pile under lateral loading, an interface element is considered to reproduce the lost contact between both materials as shown in Figure 5. The interface element, as described in previous literature (Cerfontaine, Dieudonné, Radu, Collin, & Charlier 2015) and(Cerfontaine, Collin, & Charlier 2015), belongs to the zero-thickness family:

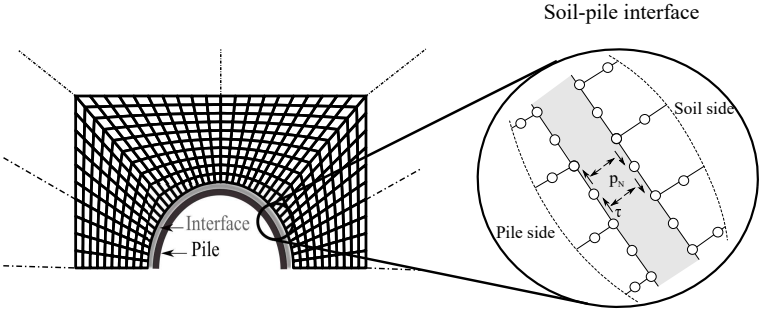

Figure 5: Interface finite element

The probable zone of contact respects the "ideal contact constraint states":

$$g_N \geq 0, \quad p_N \geq 0, \quad p_N.g_N = 0 \tag{1}$$

where p_N is the normal pressure, and g_N is the gap between two sides of the interface. This ideal constraint

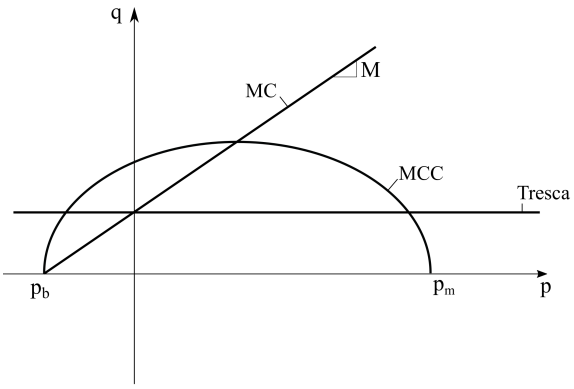

Figure 6: MCC, MC and Tresca yield surface in $p-q$ plane

establishes that contact holds if the gap is equal to zero (closed), giving rise to a normal contact pressure. Whereas, if the gap is positive (open), it indicates a non-contact pressure. The shear behavior of the interface is described similarly, in which maximum shear resistance along the interface is ruled by Mohr-Coulomb criterion, and according to:

$$\tau_{max} = \sigma_n \tan\phi \tag{2}$$

where ϕ is the steel-soil friction angle, which is equal to two thirds the shear angle of the soil.
If the shear stress is lower than τ_{max} soil and pile are considered "stuck", and the relative tangential displacement g_T is null. If the maximal shear stress is reached, both sides of interface encounter a relative displacement.

p-y curve from 2D finite element method

The soil reaction curve is extracted from the 2D simulation from post-processing routines. As illustrated in Figure 1, computed total stress (normal pressure and shear stress) in the interface elements is integrated along the pile circumference to determine the local lateral load (p), which is related to the local pile displacement (y).

Constitutive models

In order to analyze the influence of the constitutive model, with respect to simplified model such as Tresca criterion, two additional constitutive laws have been considered. The Mohr-Coulomb (MC) criterion is firstly used as a reference model for soils, secondly the Modified Cam-Clay model (MCC) is also used in the modeling. The MCC model is the first critical state model that describes the behavior of soft soils such as clay. Assuming isotropic behavior, the MCC model is defined by a yield criterion represented, in $p-q$ plane, by an ellipse oriented in line with the p axis as shown in Figure 6.
The model is described by the following equation in generalized space:

$$f\left(\sigma_d, p, p_m\right) = \frac{3}{2}\sigma_d : \sigma_d + M^2\left(p + p_b\right)\left(p - p_m\right) = 0 \tag{3}$$

σ_d is the shear stress tensor $\left(\sigma_{d_{ij}} = \sigma_{ij} - \delta_{ij}p\right)$, and p is the mean stress. M is the slope of the critical state line in $p-q$ plane. This parameter is calculated directly from the shear angle of soil ϕ, as follow:

$$M = \frac{6\sin\phi}{3-\sin\phi} \tag{4}$$

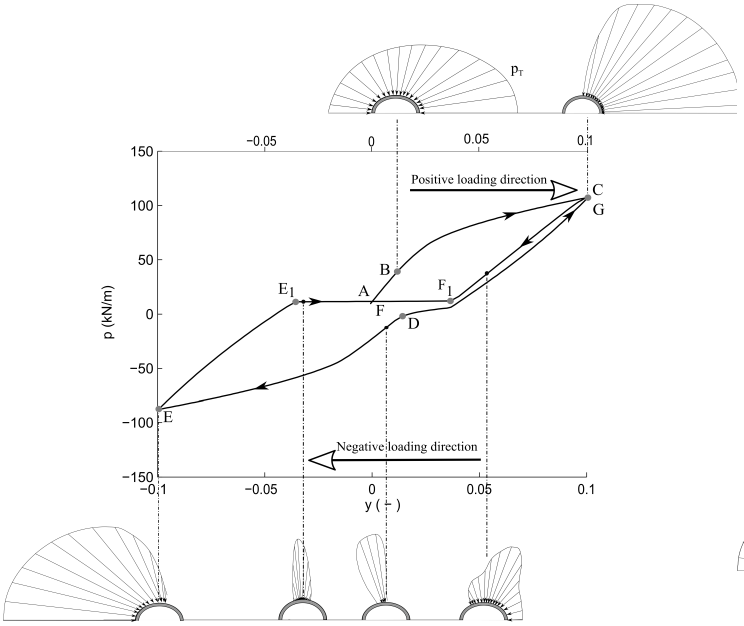

Figure 7: p-y curve and total pressure contact at $5m$ of depth

p_m represents the preconsolidation pressure of soil. It controls the size of the yield surface, due to the following isotropic hardening rule:

$$\dot{p}_m = \frac{1+e}{\lambda-\kappa} p_m \dot{\varepsilon}_v^p \tag{5}$$

where e is the current void ratio, κ and λ are the compression and swelling slope of the isotropic consolidation line in $e - \ln p$ respectively.

The set of soil properties, presented in Table 1, is considered for this analysis. The soil is assumed as a slightly overconslidated clay $(ocr = 1.2)$. In-situ stresses are estimated with an assumption of a unit weight of $15kN.m^{-3}$, and the isotropic initial conditions are respected. The chosen soil is a natural and very soft clay, representative of some marine clays such as the clay of Gulf of Mexico and the shallow clay in the North Sea (Bjerrum 1973).

Table 1: Soil parameters

	ν	κ	E (MPa)	λ	ϕ	c (kPa)	ocr
Tresca	0.25	-	2	-	0	10	-
MC	0.25	-	2	-	32	10	-
MCC	0.25	0.04	-	0.26	32	10	1.2

3 RESULTS ANALYSIS

The aim of this section is to study the influence of the interface between the soil and the pile, in addition to the soil behavior on p-y curves of laterally loaded pile.

Soil-Pile interaction

Before analyzing the behavior of different soil models, the p-y curve has been explained using one type of soil behavior model. The p-y curve is predicted by using MCC model at different depth levels, illustrated at different loading levels.

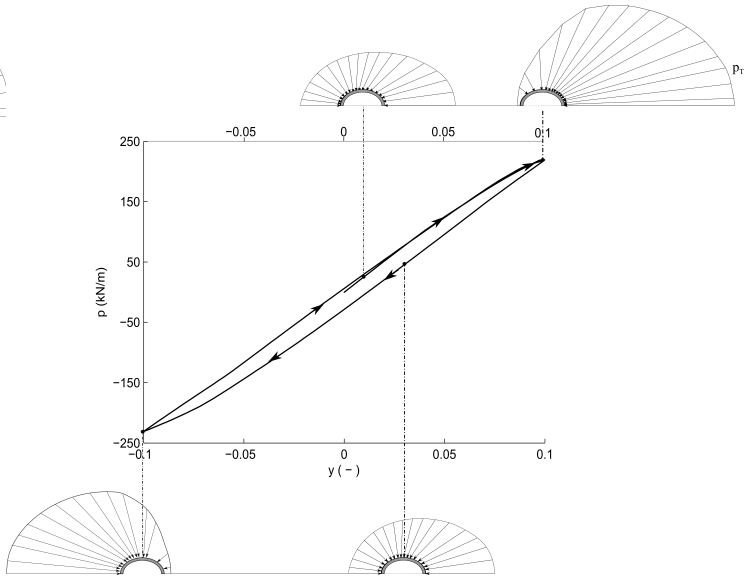

Figure 8: p-y curve and total pressure contact at $15m$ of depth

As shown in Figure 8 and 7, p-y curves are illustrated at different depths, with the distribution of the total contact pressure $p_T = p_N + \tau$ around the pile in different loading levels. Figure 8 shows the p-y curve at a depth of 5m, while Figure 7 shoes the p-y curve at a depth of 15m.

It has been observed that the evolution of the p-y curve at $5m$ of depth is going through different phases as explained below:

phase 1 (portion AB): Initially, at point A, the stresses are uniform and normal to the pile section, assuming that the foundation is vertical, and installed without inducing any initial friction. The pile loading induces a redistribution of the total pressure around the pile, shear stresses appear, and the normal pressure increase in the positive side of the pile section, and remains positive and non-null around the pile until point B. In addition, the p-y curve has a linear form.

phase 2 (portion BC): p-y curve has a non-linear form during this phase. This non linearity is related to the non-linearity of soil, and on the other hand to the non-linearity of soil-pile interface behavior. Therefore, during loading, the total pressure around the pile evolves until it reaches a null value. Thus, a gap between soil and pile appears, which is considered as an irreversible deformation, and then allows non-linear behavior of the structure. When the maximum displacement is applied (Point C), the gap reaches all the negative side, while the total pressure remains non-null in

the positive side and reaches its maximum value in front of the pile section.

phase 3 (portion CD) : The unloading phase is started. In the positive side, the soil reaction (p) decreases with unloading, until a gap appears. In the negative side, the contact pressure increases.

phase 4 (portion DE): first, the pile is loaded until its initial position, and then loaded in the negative direction up to 10% of pile diameter. During this phase, the contact pressure is increasing in the negative side, and decreasing in the positive side, until its reaches its maximum value at point E. The gap increases during this phase in the positive side.

phase 5 (portion EF): During this phase, a horizontal displacement is applied in the positive direction until its initial position. The contact pressure decreased in the negative side, and increases in the positive side. Then, the gap evolves in the negative and positive sides. Due to the gap behavior, the soil reaction (p) reaches its minimum value in the portion (E1F), where the two structures are in contact just in the head of the pile section.

phase 6 (portion FG): This section can be subdivided into two portions, the first portion (FF1, which is similar to the portion E1F, and characterized by the gap in the negative and the positive sides, and the second portion (F1G), when the gap disappears in the positive side. The segment F1G has the same form of the portion CD,during the unloading.

At 15 meters of depth, the distribution of contact pressure remains non-null around the pile during loading and unloading phases. The resulted p-y curve has continuous form, without any slop break.

As shown in Figures 8 and 7, the p-y curve has entirely different form compared to the extracted curve in 5 meters of depth. The resulted p-y curves have different evolutions due to two main reasons. The first reason is related to the depth of the analyzed surface, while the second reason is due to the soil-pile interface behavior resulting from the lateral loading on the pile. However, the consequence of the soil-pile interface behavior highly differs from one depth to another. For instance, at the depth of 5 meters, lateral loading shifts the soil together with the pile. This shift causes a redistribution of the contact pressure around the pile and creates a gap between the soil and the pile. Thus, a null value is obtained for the total contact pressure as a result of that gap. However, the same loading does not induce a gap at a depth of 15 meters, it only redistributes the contact pressure. From this analysis, it is concluded that the evolution of the lateral capacity (p) at a certain depth is entirely related to the soil behavior.

Influence of the constitutive model

The main objective of this section is to assess the influence of soil behavior on the p-y curve. For this reason, three soil models, Tresca, Mohr-Coulomb (MC) and Modified Cam-Clay model (MCC) have been chosen for the modelling, the mesh and boundary conditions remaining the same as described in the section 2. The considered soil parameters for each constitutive law are given in Table 1. The extracted p-y curves

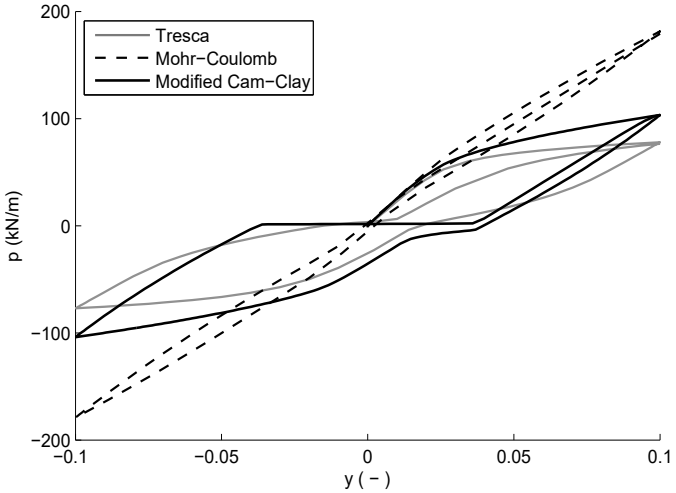

Figure 9: p-y curves at 5m of depth

are illustrated in Figure 9 at the same depth of 5 meters. At this depth, it is observed that the p-y curve behaves similarly, in terms of pile interface behavior, for the different soil models as shown in the Figure 9. Pile interface behavior is characterized by the gap formation between the two materials (soil and pile). However, the impact of different soil behaviors appears in the mobilization of the pile lateral capacity.

It has been observed that Mohr-Coulomb model has the highest mobilization effect of contact pressures. MC induces a higher value of lateral capacity compared to the MCC and Tersca models. This difference is explained by the elastic domain predicted by each model. For instance, MC model has a larger elastic domain compared to Tresca criterion as shown in Figure 5. With the MCC, the soil is considered normally consolidated, which means that the soil reached the plasticity state once loading path. High elastic domains correspond to high values of lateral capacity.

It has been observed from the same Figure that MCC model predicts higher value of lateral capacity compared to Tresca prediction. On one hand, Tresca model is an elastic perfectly-plastic model. While on the other hand, MCC predicts the hardening and softening states of the soil. For slightly overconsolidating soil (with $ocr = 1.2$), hardening phase occurs rapidly while elastic limit increases constantly with increasing the loads.

Figure 10 shows different soil zones where the plasticity is reached in the case of Tresca, MC and MCC simulations at $10\%D$ of horizontal displacement in the positive side. For the three simulations,the soil

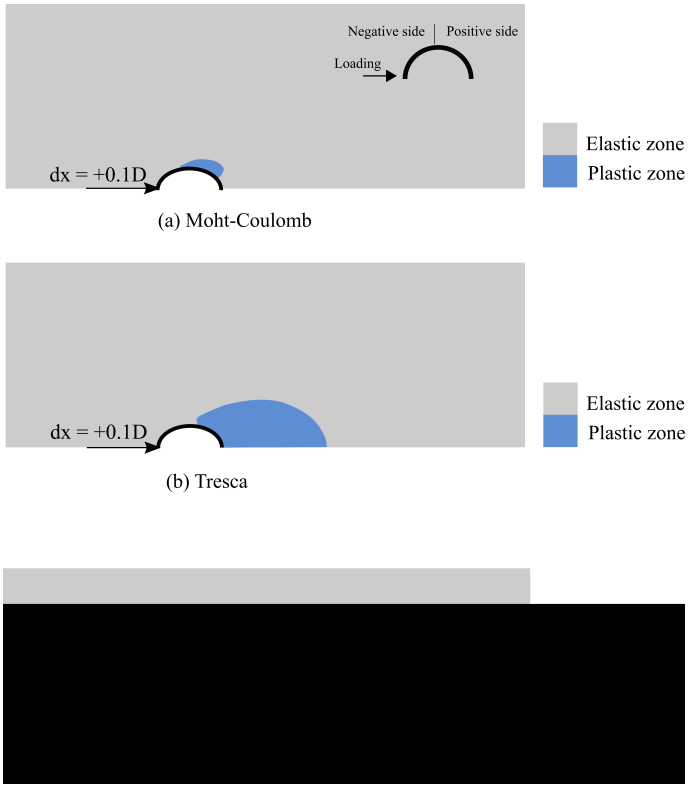

Figure 10: Plasticity zones for $10\%D$ of lateral displacement

plasticity evolves during loading, but not with the same extent: the simulated soil with MC model remains elastic around the pile except at the pile head where plastic strains appears. In the case of MCC model, the plasticity is reached around the pile once the horizontal displacement is applied, because of the assumption of slightly overconsolidating soil. While the soil is in plasticity just in the positive side in the case of Tresca model. These observations support the interpretations that it has been done from Figure 9.

4 CONCLUSIONS

The laterally loaded pile has been investigated in this article, in which Tresca, Mohr-Coulomb, and Modified Cam-Clay models have been applied during the investigation. Those soil models are considered to be the most widely used in laterally loaded pile modeling. Moreover, the interface impact was outlined, and the gapping phenomenon was explained at different depths of the pile.

The extracted p-y curves have shown critical differences related to the soil behavior. It has been observed that Tresca criterion underestimates the soil capacity compared to Mohr-Coulomb and Modified Cam-Clay models, and Mohr-Coulomb criterion predicts high value of lateral capacity compared to other models. This remarks have been related directly to the evolution of soil plasticity during loading. While MC and Tresca models are elastic perfectly plastic models, MCC model predicts some soil hardening. Moreover, MC model allows a large elastic domain compared to Tresca criterion.

The analyzed results are based on 2D simulation with the assumption of plane deformation. However, it should be noted that laterally loaded pile is actually a 3D problem. The assumption of plane strain remains only relevant for certain depth, which is considered to be one limitation in this research. In fact, two soil mechanisms may exist in the soil resistance for laterally loaded pile as explained in (Reese, Cox, & Koop 1974). In the upper part, soil fails in a conical wedge that extends to the soil surface. The soil failure mechanism transits into a localized plane mechanism at a certain depth. Therefore, 3D simulations are recommended to be provided within further research. Moreover, a complete cyclic load is recommended to be calculated to investigate the interface behavior in later stages of cyclic load.

REFERENCES

Ahayan, S., Z. Yin, P. Kotronis, & F. Collin (2016). L'effet de l'écrouissage rotationnel sur le comportement des sols argileux. In *34émes Rencontres de l'AUGC*. University of Liège.

Arshad, M. & B. C. OKelly (2013). Offshore wind-turbine structures: a review. *Proceedings of the Institution of Civil Engineers-Energy 166*(4), 139–152.

Bjerrum, L. (1973). Problems of soil mechanics and construction on soft clays and structurally unstable soils (collapsible, expansive and others). In *Proc. of 8th Int. Conf. on SMFE*, Volume 3, pp. 111–159.

Byrne, B., R. McAdam, H. Burd, G. Houlsby, C. Martin, L. Zdravkovi, D. Taborda, D. Potts, R. Jardine, & M. Sideri (2015). New design methods for large diameter piles under lateral loading for offshore wind applications. In *3rd International Symposium on Frontiers in Offshore Geotechnics (ISFOG 2015), Oslo, Norway, June*, pp. 10–12.

Cerfontaine, B., F. Collin, & R. Charlier (2015). Numerical modelling of transient cyclic vertical loading of suction caissons in sand. *Géotechnique 65*(12).

Cerfontaine, B., A.-C. Dieudonné, J.-P. Radu, F. Collin, & R. Charlier (2015). 3d zero-thickness coupled interface finite element: formulation and application. *Computers and Geotechnics 69*, 124–140.

EWEA, E. (2015). The european offshore wind industry key trends and statistics 1st half 2015. *European Wind Energy Association (EWEA) 1*, 8.

EWEA, E. (2017). The european offshore wind industry- key trends and statistics 2016. *European Wind Energy Association (EWEA) 1*, 8.

Matlock, H. (1970). Correlations for design of laterally loaded piles in soft clay. *Offshore Technology in Civil Engineerings Hall of Fame Papers from the Early Years*, 77–94.

Randolph, M. F. & G. Houlsby (1984). The limiting pressure on a circular pile loaded laterally in cohesive soil. *Geotechnique 34*(4), 613–623.

Reese, L. C., W. R. Cox, & F. D. Koop (1974). Analysis of laterally loaded piles in sand. *Offshore Technology in Civil Engineering Hall of Fame Papers from the Early Years*, 95–105.

Roscoe, K. & J. Burland (1968). On the generalized stress-strain behaviour of wet clay.

RP2A-WSD, A. (2000). Recommended practice for planning, designing and constructing fixed offshore platforms–working stress design–. In *Twenty-*.

Schaumann, P., S. Lochte-Holtgreven, & S. Steppeler (2011). Special fatigue aspects in support structures of offshore wind turbines. *Materialwissenschaft und Werkstofftechnik 42*(12), 1075–1081.

Veritas, D. N. (2004). Design of offshore wind turbine structures.

Offshore Standard DNV-OS-J101 6, 2004.

Zdravković, L., D. Taborda, D. Potts, R. Jardine, M. Sideri, F. Schroeder, B. Byrne, R. McAdam, H. Burd, G. Houlsby, et al. (2015). Numerical modelling of large diameter piles under lateral loading for offshore wind applications. In *Proceeding 3rd International Symposium on Frontiers in Offshore Geotechnics. Norway:[sn]*.

Zhang, F., B. Ye, T. Noda, M. Nakano, & K. Nakai (2007). Explanation of cyclic mobility of soils: Approach by stress-induced anisotropy. *Soils and Foundations 47*(4), 635–648.